A refactored biosynthetic pathway for the production of glycosylated microbial sunscreens

Sıla Arsın[1], Maija Pollari[1,3], Endrews Delbaje[2], Jouni Jokela[1], Matti Wahlsten[1], Perttu Permi[4, 5], David Fewer[1]

[1] Department of Microbiology, Faculty of Agriculture and Forestry, University of Helsinki, 00014 Helsinki, Finland.

[2] Faculdade de Ciências Farmacêuticas de Ribeirão Preto, Universidade de São Paulo, Ribeirão Preto, Brazil

[3] Department of Agricultural Sciences, Faculty of Agriculture and Forestry, University of Helsinki, 00014 Helsinki, Finland.

[4]Department of Chemistry, University of Jyväskylä, 40014 Jyväskylä, Finland

[5]Department of Biological and Environmental Science, Nanoscience Center, University of Jyväskylä, 40014 Jyväskylä, Finland

*Corresponding author

E-mail address: david.fewer@helsinki.fi

Supplementary Information

Table of Contents

Table S1. MAA intermediates and variants detected from *Nostoc* sp. UHCC 0302 by HR-LCMS based on their UV absorbtion at 320 nm and their abundance is based on the area of absorbtion in percentages (Area %). Retention time: RT, (experimental) *m/z* in [M+ H] $^{+}$. (Hexose: Hex, Pentose: Pen, Galactose: Gal, Glucose: Glu, Xylose: Xyl)

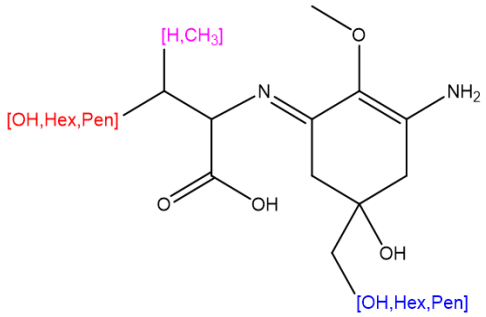

#	MAA	RT (min)	*m/z*	Area (320nm)	Area (%)
1	Thr-4DG-NH_2- Xyl	6.40	421.18	197	6.4
2	Xyl-Thr-4DG-NH_2	6.61	421.18	32	1.1
3	Ser-4DG-NH_2-Xyl	6.82	407.17	377	12.3
4	Thr-4DG-NH_2-Glc	7.10	451.19	549	17.8
5	Gal-Thr-4DG-NH_2- Xyl	7.79	583.24	320	10.4
6	Gal-Ser-4DG-NH_2- Xyl	8.22	569.22	1602	52.1

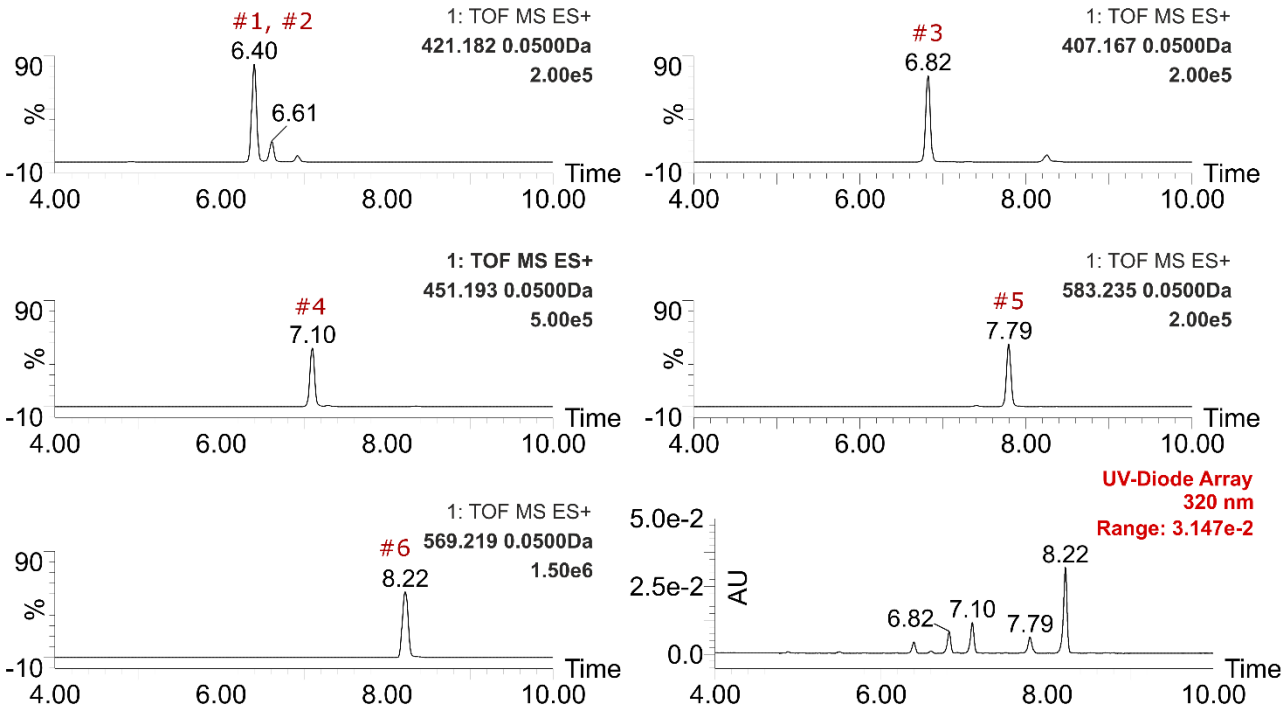

Figure S1. MS-ES^{+} and UV (320 nm) chromatograms showing the detected MAA intermediates and variants from the *Nostoc* sp. UHCC 0302 methanol extracts.

Table S2. Product ions of 568 Da MAA from MS^E spectrum. Codes are marked to the 568 Da MAA molecule in Figure S2. Δ = difference of calculated (Calc) and experimental (Exp) ion masses in parts per million (ppm).

Product ion			*m/z*		
code		**Neutral loss**	**Calc**	**Exp**	**Δ (ppm)**
	$[M+K]^+$		607.1747	607.1732	-2.5
	$[M+Na]^+$		591.2008	591.1999	-1.6
	$[M+H]^+$		569.2188	569.2195	1.1
a	$[M+H]^+$	$CH_3^{\cdot}$	554.1954	554.1943	-2.0
b	$[M+H]^+$	CH_2O	539.2083	539.2081	-0.4
b	$[M+H]^+$	CH_3OH	537.1926	537.1922	-0.9
c	$[M+H]^+$	$C_2H_2N^{\cdot}$	529.2001	529.2005	0.6
d	$[M+H]^+$	CO_2	525.2290	525.2291	0.1
d	$[M+H]^+$	HCOOH	523.2134	523.2139	0.9
e	$[M+H]^+$	$C_4H_8O_4$	449.1766	449.1751	-3.4
f	$[M+H]^+$	Xyl	437.1766	437.1759	-1.7
g	$[M+H]^+$	Gal	407.1660	407.1659	-0.4
a-g	$[M+H]^+$	Gal, $CH_3^{\cdot}$	392.1426	392.1420	-1.5
h	$[M+H]^+$	Gal, H_2O	389.1555	389.1542	-3.4
b-g	$[M+H]^+$	Gal, CH_2O	377.1555	377.1546	-2.4
d-g	$[M+H]^+$	Gal, HCOOH	361.1605	361.1594	-3.3
d-h	$[M+H]^+$	Gal, CO_2, H_2O	345.1656	345.1649	-2.3
b-d-g	$[M+H]^+$	Gal, HCOOH, CH_2O	331.1500	331.1490	-3.1
i	$[M+H]^+$	$GalOC_3H_3O_2$	319.1500	319.1487	-4.2
i	$[M+H]^+$	$GalOC_3H_5O_2$	317.1343	317.1337	-2.1
b-i	$[M+H]^+$	$GalOC_3H_3O_2$, $CH_3^{\cdot}$	304.1265	304.1259	-2.1
f-g	$[M+H]^+$	Gal, Xyl	275.1238	275.1239	0.3
a-f-g	$[M+H]^+$	Gal, Xyl, $CH_3^{\cdot}$	260.1003	260.1001	-0.9
f-h	$[M+H]^+$	Gal, Xyl, H_2O	257.1132	257.1131	-0.6
b-f-g	$[M+H]^+$	Gal, Xyl, CH_2O	245.1132	245.1130	-1.0
b-f-g	$[M+H]^+$	Gal, Xyl, CH_3OH, $2xH_2O$	207.0764	207.0768	1.6
b-f-j	$[M+H]^+$	GalOCH, Xyl, CH_2O, H_2O	197.0921	197.0918	-1.6
f-i	$[M+H]^+$	$GalOC_3H_3O_2$, Xyl, 2H	185.0921	185.0921	-0.1
a-f-i	$[M+H]^+$	$GalOC_3H_3O_2$, Xyl, CH3$^{\cdot}$	172.0842	172.0845	1.2
	$[M+H]^+$	$C_{13}H_{28}O_{14}$	161.0709	161.0714	2.5

Table S3. NMR data of 568 Da MAA in D_2O.

No	δ_H	mult., *J*(Hz)	δ_C	HMBC
Palythine-serine				
1	-		160.9	
2	-		125.1	
3	-		160.9	
4*	2.80		34.1	2, 3, 5, 6
5	-		70.6	
6*	2.70		36.0	1, 2, 4, 5, 7
7a	3.43	d, 10.0	73.3	5, 6, 1'
7b	3.72	d, 10.1		5, 6, 1'
8	3.64	s	59.4	2
9	4.44	dd, 6.2, 3.6	59.0	3, 10, 11
10	-		174.3	
11a	4.03	dd, 11.0, 3.5	70.3	9, 10, 1"
11b	4.29	dd, 11.0, 6.2		9, 10, 1"
α-D-xylopyranose				
1'	4.89	d, 3.7	98.9	5', 7
2'	3.54		71.7	3'
3'	3.65		73.3	2', 4'
4'	3.60		69.6	3', 5'
5a'	3.45		61.6	1', 3', 4'
5b'	3.70			1', 3', 4'
β-D-galactopyranose				
1"	4.37	d, 8.0	103.2	2", 3", 5", 11
2"	3.49		70.9	1", 3"
3"	3.61		72.9	2"
4"	3.87	dd, 0.8, 3.3	68.9	2", 3"
5"	3.64		75.5	1", 4", 6"
6a"	3.69		61.3	4", 5"
6b"	3.74			4", 5"

* = 4 and 6 signals can be interchanged.

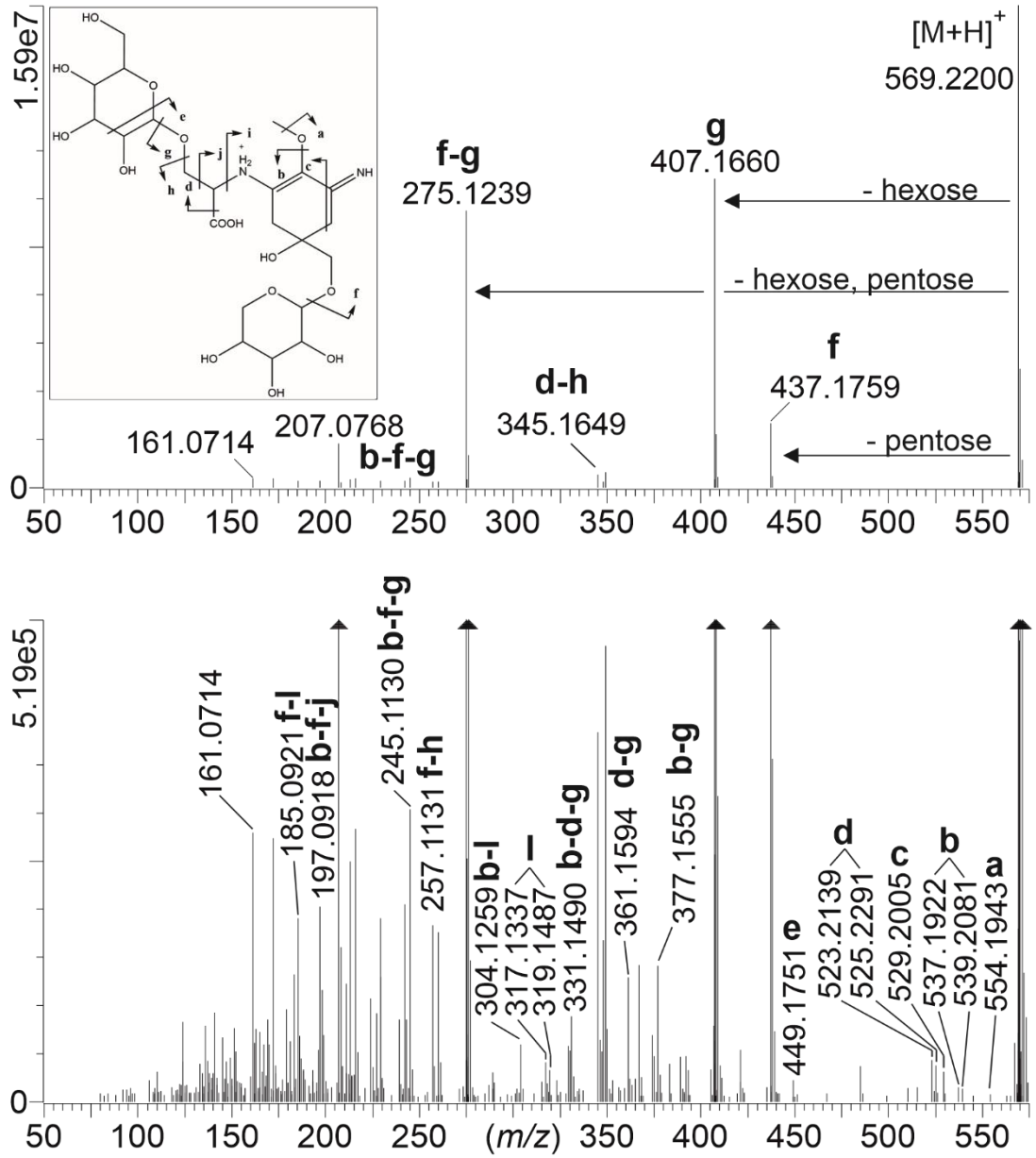

Figure S2. Product ion spectrum of protonated 568 Da MAA. The lower panel shows the low intensity ions.

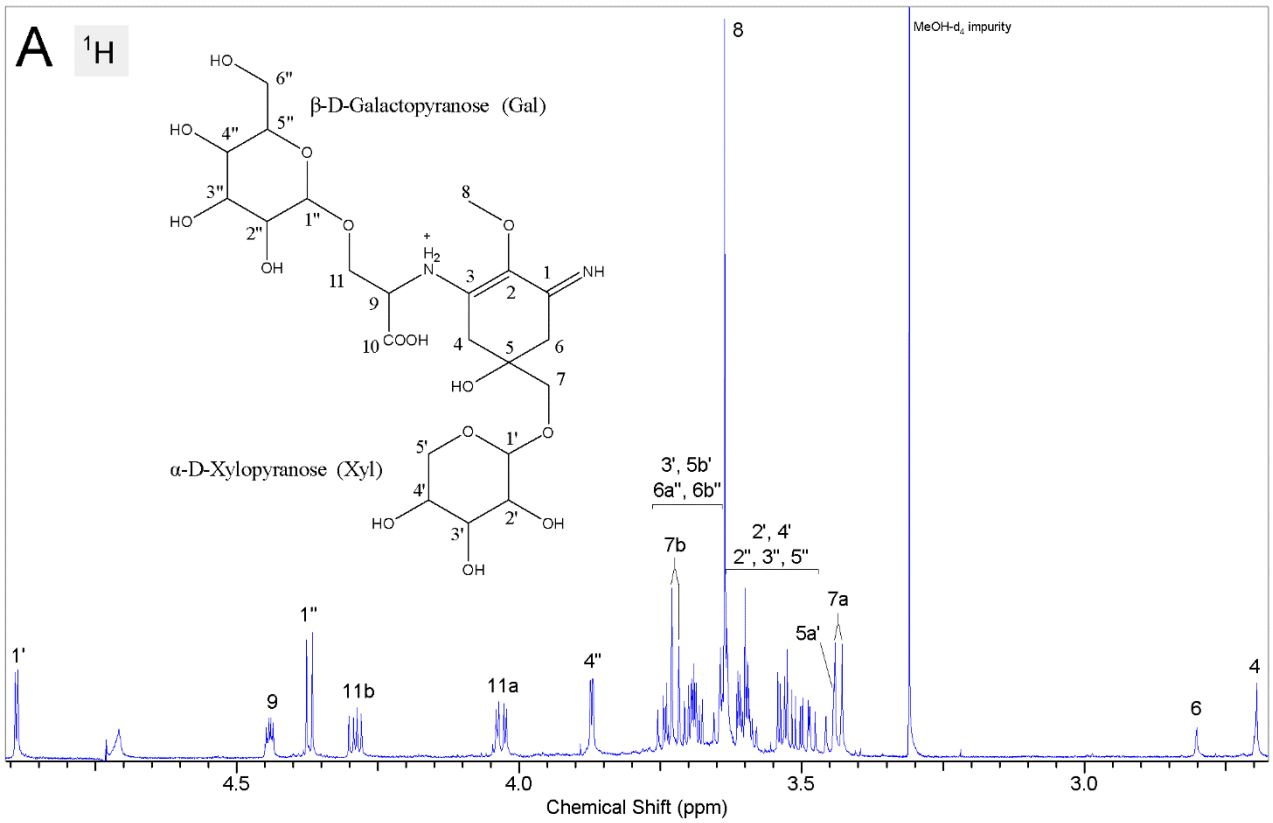

Figure S3. Partly annotated proton spectrum of 568 Da MAA in D_2O.

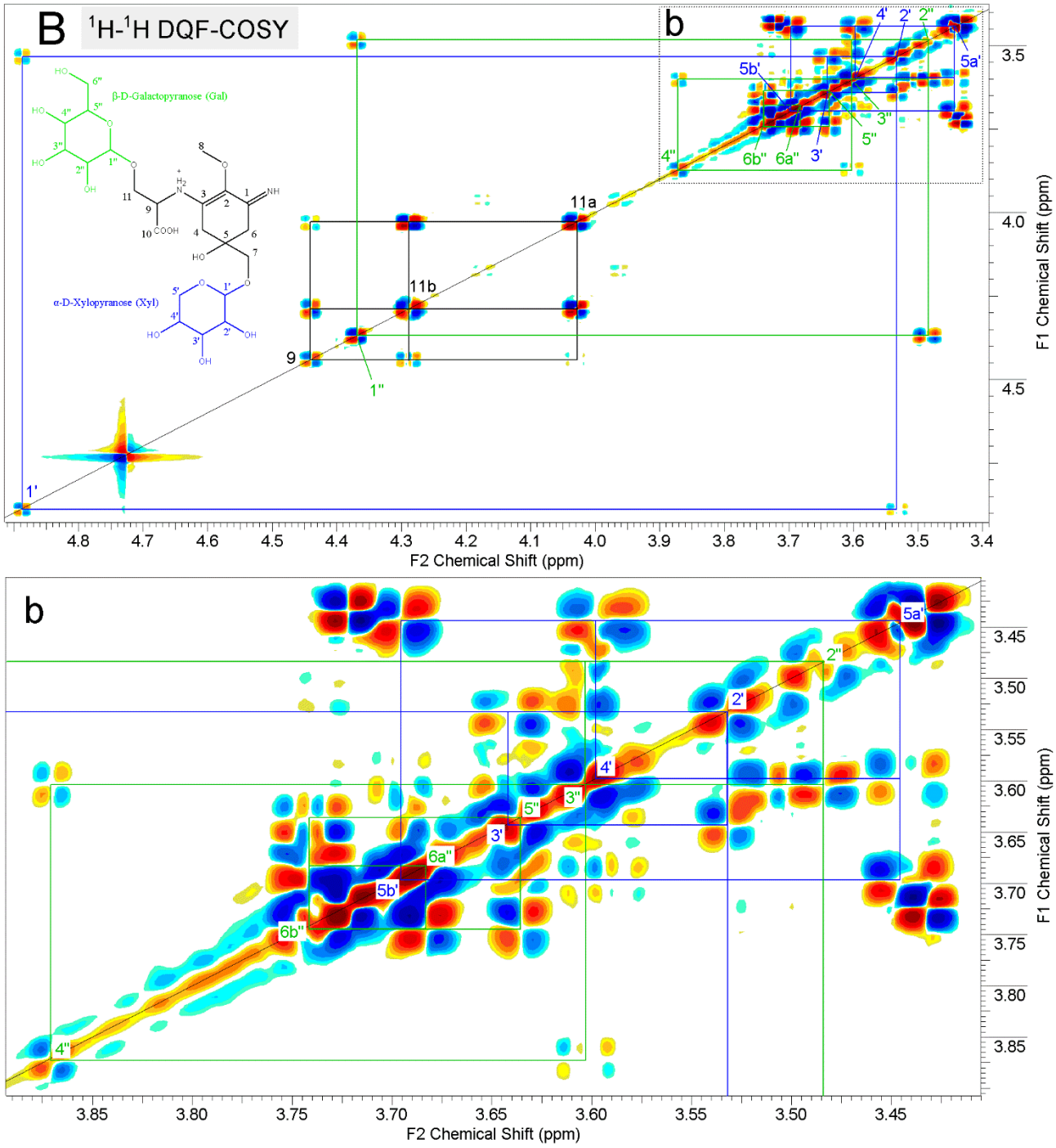

Figure S4. Annotated ^{1}H-^{1}H DQF-COSY spectrum of 568 Da MAA in D_2O with enlargement from area b.

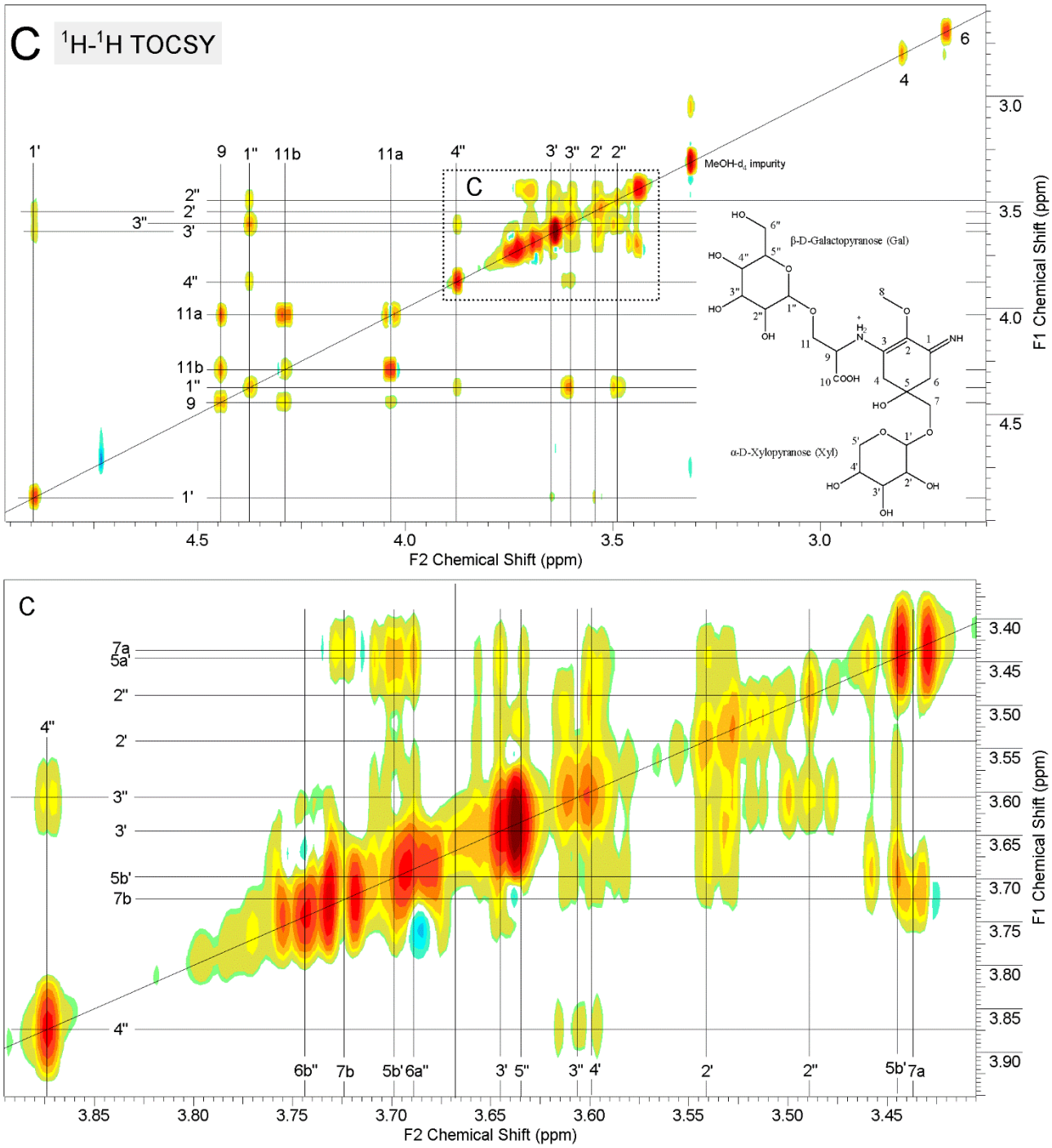

Figure S5. ^{1}H-^{1}H TOCSY (90 ms) spectrum of 568 Da MAA in D_2O.

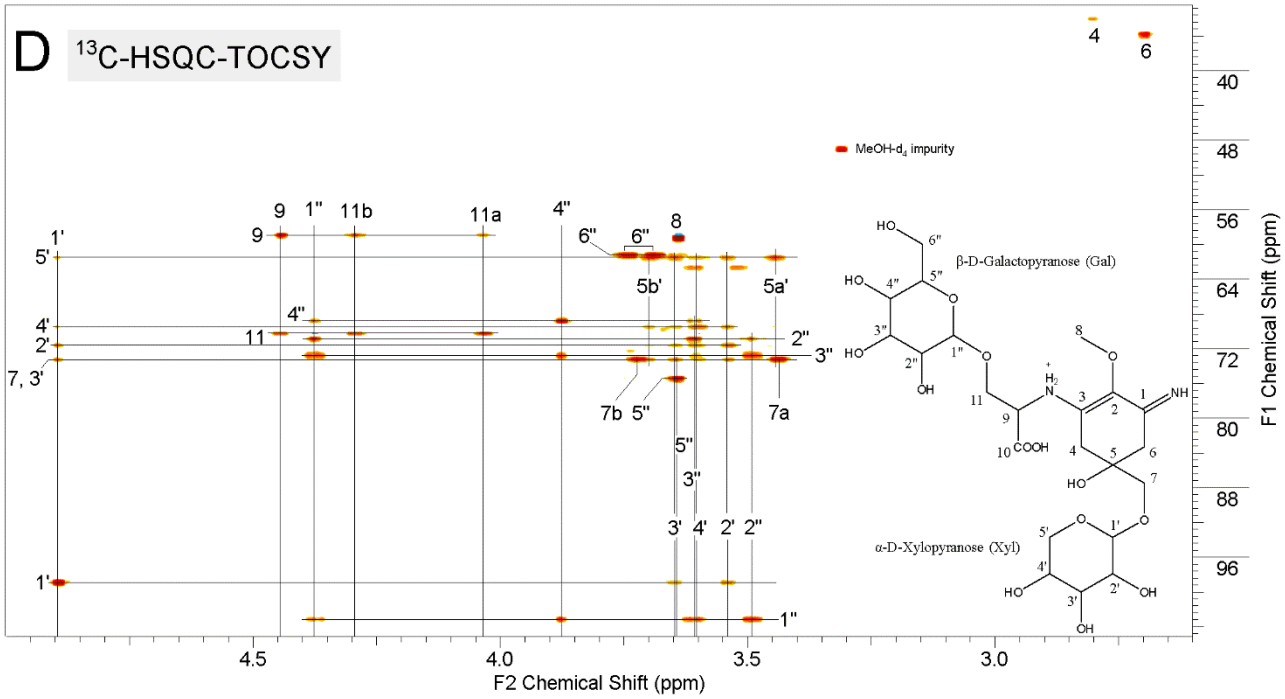

Figure S6. Annotated ^{13}C-HSQC-TOCSY spectrum of 568 Da MAA in D_2O.

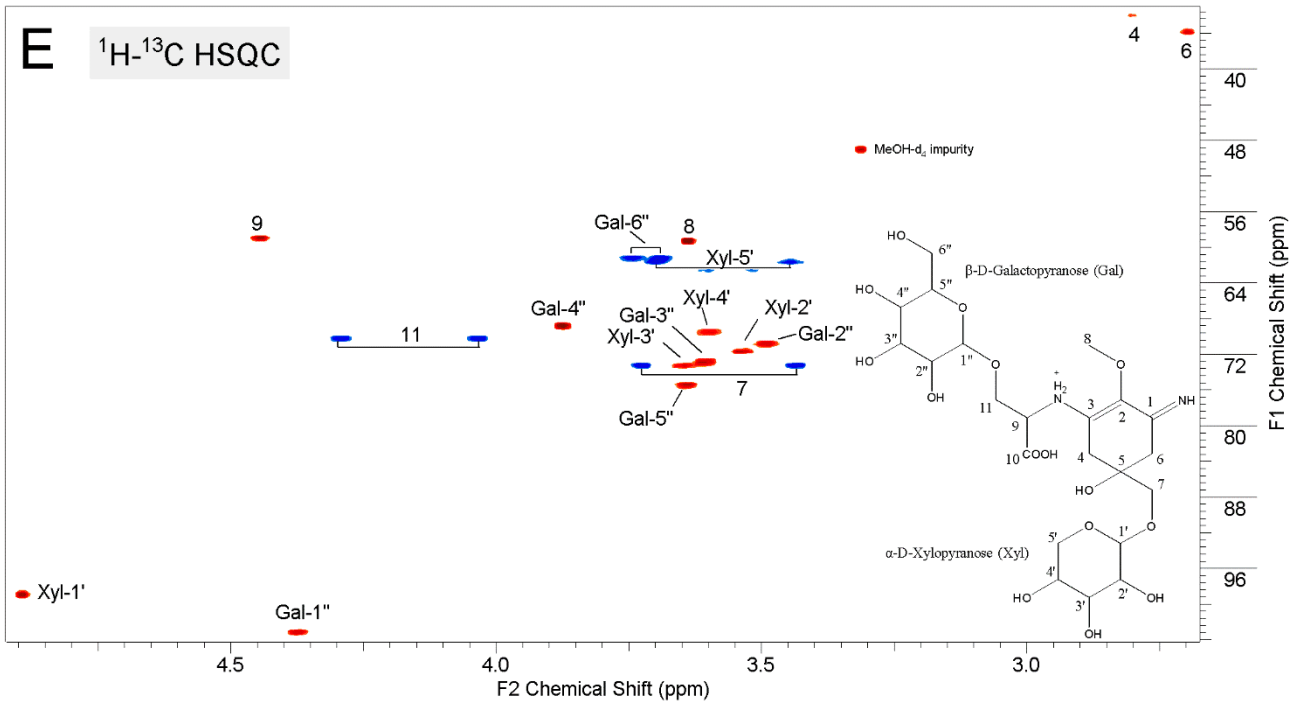

Figure S7. Annotated edited ^{1}H-^{13}C HSQC spectrum of 568 Da MAA in D_2O.

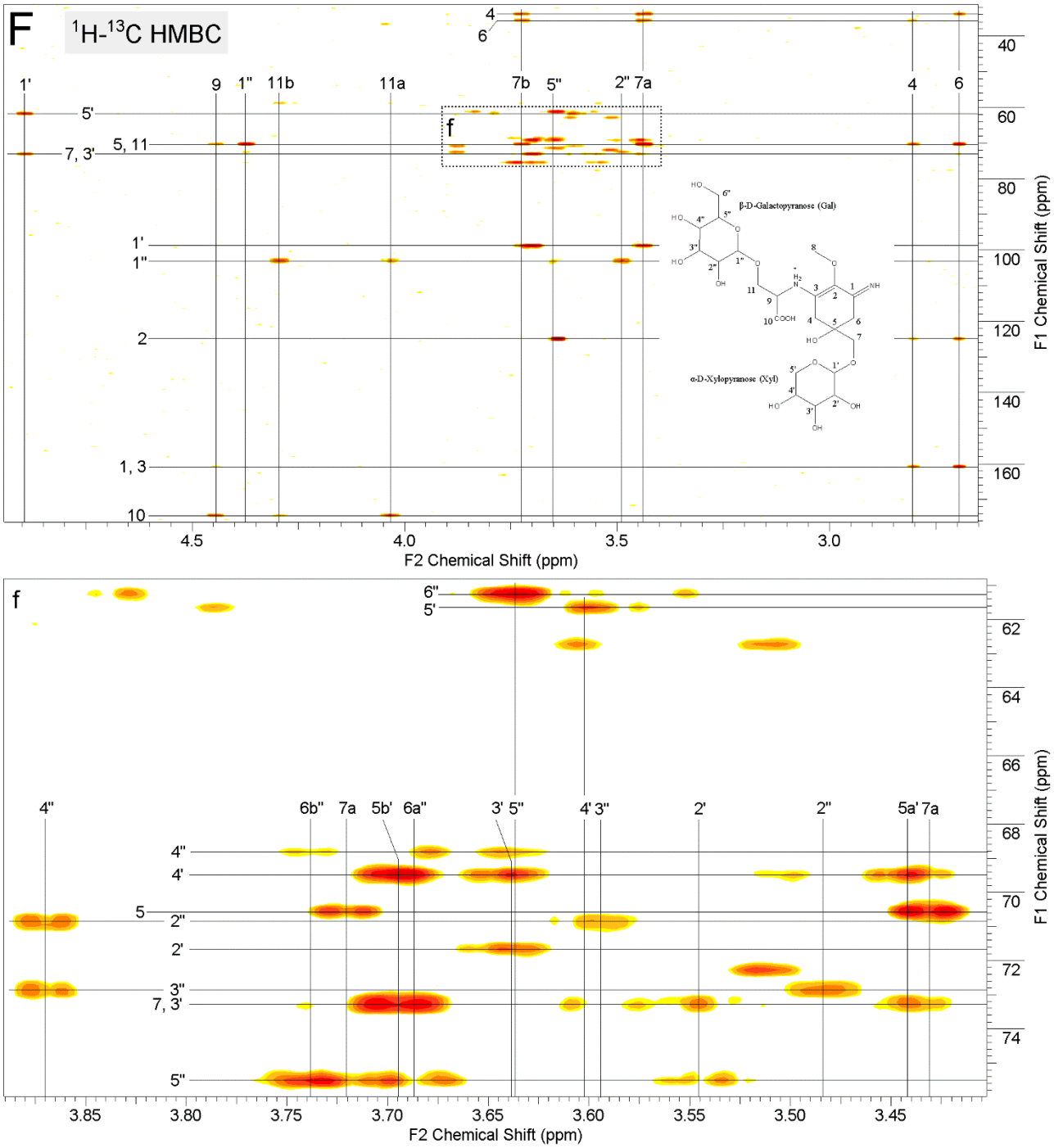

Figure S8. Annotated ^{1}H-^{13}C HMBC spectrum of 568 Da MAA in D_2O with enlargement from area f.

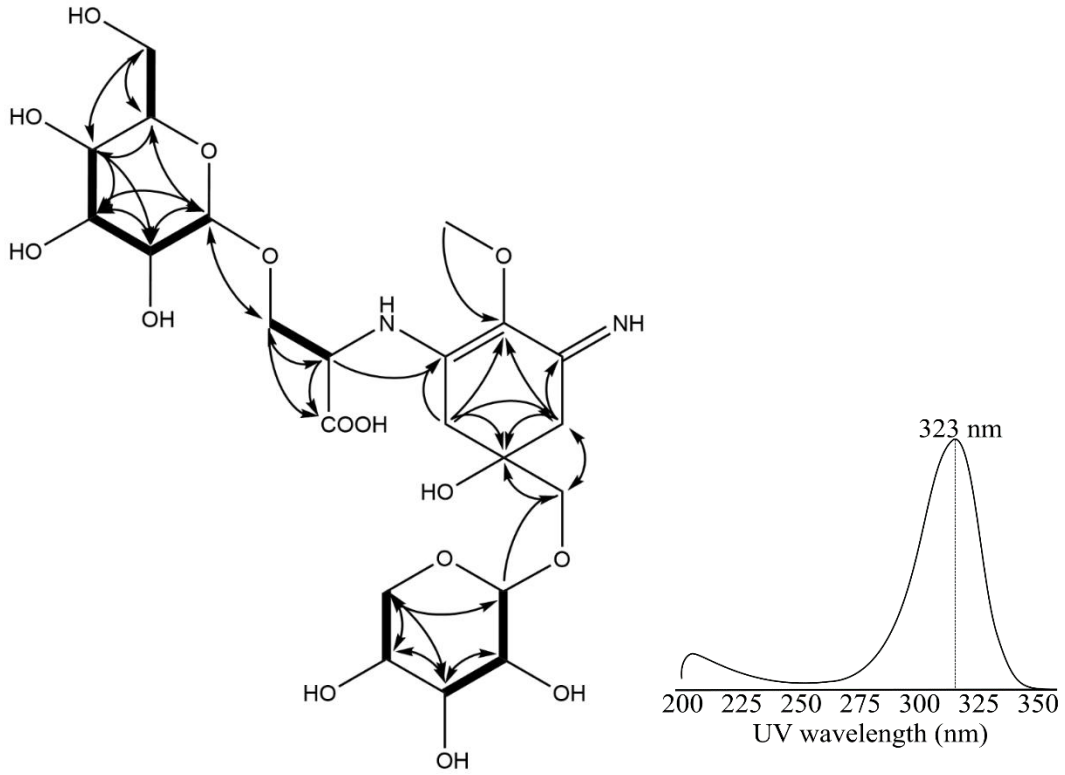

Figure S9. HMBC and COSY correlations of 568 Da MAA, and its absorbtion maxima at 323 nm.

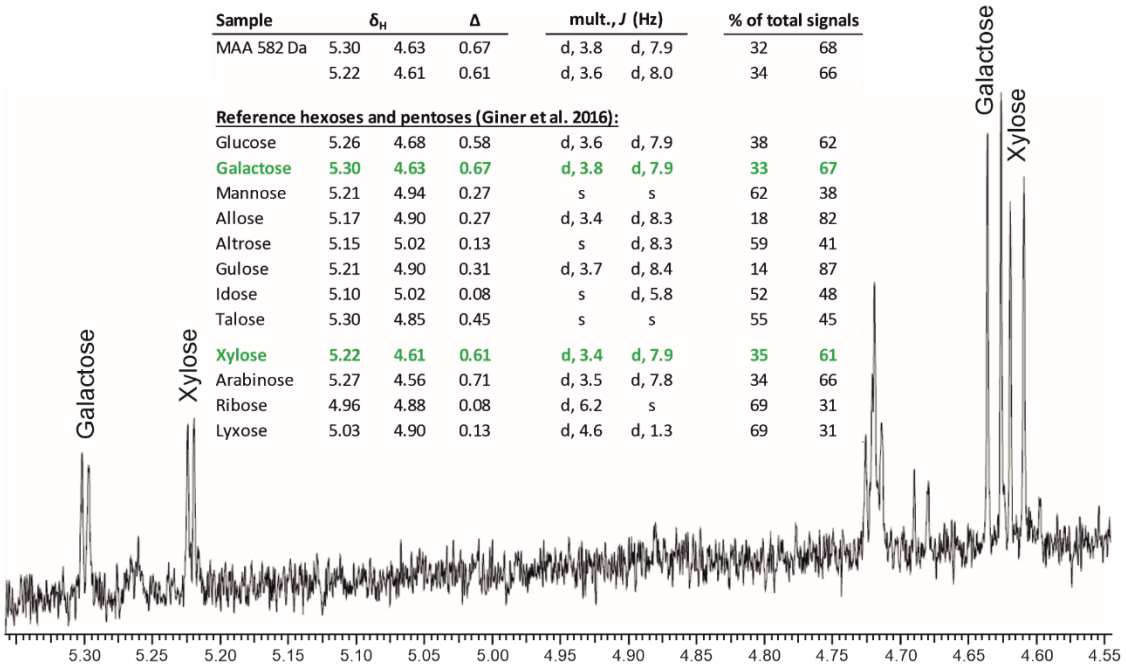

Sample	δ_H		Δ	mult., *J* (Hz)		% of total signals	
MAA 582 Da	5.30	4.63	0.67	d, 3.8	d, 7.9	32	68
	5.22	4.61	0.61	d, 3.6	d, 8.0	34	66
Reference hexoses and pentoses (Giner et al. 2016):							
Glucose	5.26	4.68	0.58	d, 3.6	d, 7.9	38	62
Galactose	**5.30**	**4.63**	**0.67**	**d, 3.8**	**d, 7.9**	**33**	**67**
Mannose	5.21	4.94	0.27	s	s	62	38
Allose	5.17	4.90	0.27	d, 3.4	d, 8.3	18	82
Altrose	5.15	5.02	0.13	s	d, 8.3	59	41
Gulose	5.21	4.90	0.31	d, 3.7	d, 8.4	14	87
Idose	5.10	5.02	0.08	s	d, 5.8	52	48
Talose	5.30	4.85	0.45	s	s	55	45
Xylose	**5.22**	**4.61**	**0.61**	**d, 3.4**	**d, 7.9**	**35**	**61**
Arabinose	5.27	4.56	0.71	d, 3.5	d, 7.8	34	66
Ribose	4.96	4.88	0.08	d, 6.2	s	69	31
Lyxose	5.03	4.90	0.13	d, 4.6	d, 1.3	69	31

Figure S10. Partial ^{1}H spectra of 568 Da MAA acid hydrolysate in 2 M D_2SO_4 (in D_2O) showing the match of anomeric protons signals to reference compounds presented in the table which values are from Giner et al., J Nat Prod 2016, 79, 2413-2417.

Structural characterization of 450 Da hexose-palythine-threonine purified from *E. coli* BL21 (DE3) expressing the *mysABCJ$_1$D$_1$HG$_1$*::pET28a+

High resolution QTOF-MS gave elemental composition of $C_{18}H_{30}N_2O_{11}$ (*m/z* 451.1919 for $[M+H]^+$, Δ − 0.7 ppm) for the neutral 450 Da MAA compound. Fragmentation of the protonated molecule (Fig. S11, Table S5), UV maximum of 323 nm (Fig. S12) together with published MAA structural data indicate that the structure of 450 Da MAA is palythine-threonine (PT) with a hexose unit in 7-OH as presented in Figure S12. To get confirmation for the structure, 450 Da MAA was purified for NMR analysis. Sample was dissolved to D_2O and ^1H, ^1H-^1H DQF-COSY, edited ^1H-^{13}C HSQC and ^1H-^{13}C HMBC spectra were recorded. Numerical data is presented in Table S6 and spectra in Figures S13-17. All δ_H and δ_C signals and COSY/HMBC correlations for atom positions 1-12 were typical for palythine-threonine structure (Table S6). Also signals from a hexose (Hex) unit were recognized. HMBC correlation from PT H-7 and Hex anomeric C-1 was present meaning that Hex is connected to the PT unit 7-OH (Fig. S12). All δ_H and δ_C Hex signals and coupling constant $^3J_{H1,H2}$ of 3.7 Hz and $^1J_{H1,C1}$ of 170 Hz match with α-D-glycopyranose structure.

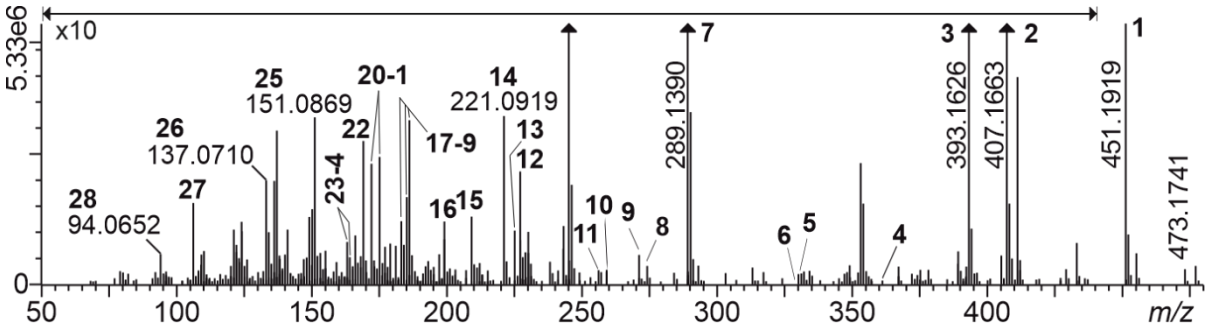

Figure S11. MS^E (E: elevated collision energy) of protonated 450 Da MAA. Codes are marked to the 450 Da MAA molecule in Figure S11. The two headed horizontal arrow shows the 10 times magnified area.

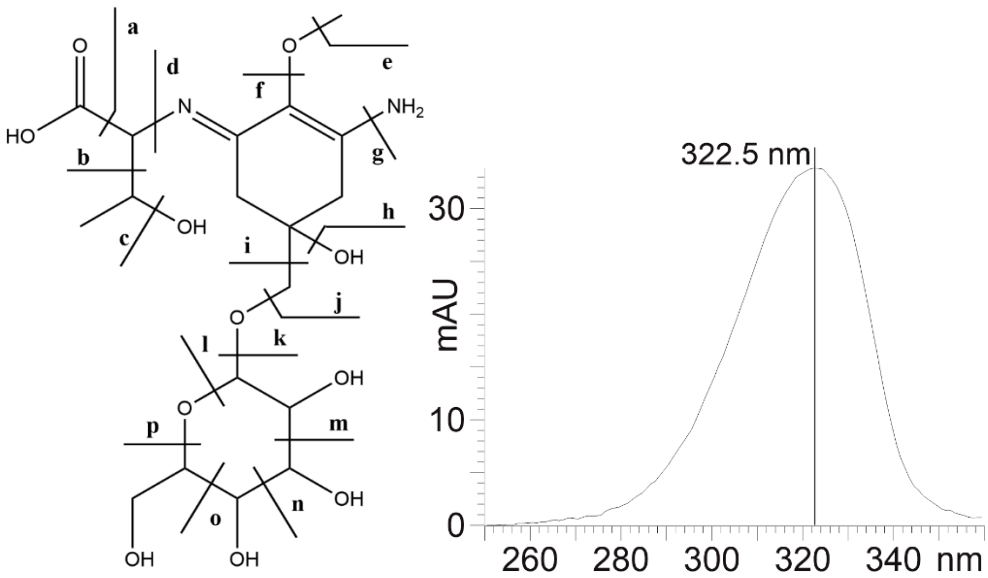

Figure S12. Ion coding marked to the 450 Da MAA structure (A). UV spectrum of 450 Da MAA from chromatoghaphic peak eluting in acetonitrile/0.2 % ammonium acetate in ratio 2/1 (B).

Table S5. Product ions of 450 Da MAA from MS^E (E: elevated collision energy) spectrum. Codes are marked to the 450 Da MAA molecule in Figure S12. Δ = difference of calculated (Calc) and experimental (Exp) ion masses in parts per million (ppm).

	Product ion		*m/z*		
No	**Code**	**Neutral loss**	**Calc**	**Exp**	**Δ (ppm)**
1		-	451.19223	451.1919	-0.7
2	o-p	C_2H_4O	407.16602	407.1663	0.6
3	g-o-p	$C_2HO^{\cdot}$, NH_3	393.16295	393.1626	-1.0
4	l-n	$C_3H_6O_3$	361.16054	361.1584	-6.1
5	l-m	$C_4H_8O_4$	331.14998	331.1486	-4.3
6	l-m	$C_4H_{10}O_4$	329.13433	329.1335	-2.7
7	k	Glc	289.13941	289.1390	-1.6
8	e-k	Glc, $CH_3^{\cdot}$	274.11594	274.1154	-2.2
9	j	Glc-OH	271.12885	271.1284	-1.8
10	i	Glc-OCH	259.12885	259.1282	-2.7
11	f-k	Glc-2H, $CH_3O^{\cdot}$	256.10537	256.1042	-4.8
12	d-l-m	$C_4H_8O_3$, $C_4H_8O_4$	227.10263	227.1025	-0.8
13	d-l-m	$C_4H_8O_3$, $C_4H_{10}O_4$	225.08698	225.0867	-1.5
14	c-h-i	Glc-OCH_3, 2 x H_2O	221.09207	221.0919	-1.0
15	f-h-i	Glc-OCH_3, CH_2O, H_2O	209.09207	209.0918	-1.5
16	a-b-k	Glc, $C_3H_6O_3$	199.10772	199.1072	-2.9
17	d-k	Glc, $C_4H_7O_3^{\cdot}$	186.09989	186.1001	0.9
18	d-k	Glc, $C_4H_8O_3$	185.09207	185.0925	2.1
19	d-k	Glc-2H, $C_4H_8O_3$	183.07642	183.0766	0.7
20	a-c-h-i	Glc-OCH_3, HCOOH, 2 x H_2O	175.08659	175.0865	-0.8
21	d-e-k	Glc, $C_4H_8O_3$, $CH_3^{\cdot}$	172.08424	172.0844	0.6
22	d-j	Glc-OH, $C_4H_6O_3$	169.09715	169.0970	-1.2
23	a-f-h-i	Glc-OCH_3, CO_2, $CH_3O^{\cdot}$, H_2O	164.09441	164.0944	-0.4
24	a-b-h-j	Glc-OH, $C_3H_6O_3$, H_2O	163.08659	163.0869	1.6
25	d-h-j	Glc-OH, $C_4H_6O_3$, H_2O	151.08659	151.0869	1.7
26	d-h-i	Glc-OCH_3, $C_4H_6O_3$, H_2O	137.07094	137.0710	0.1
27	d-f-g-h-j	Glc-O, Thr, CH_2O, H_2O	106.06513	106.0651	-0.8
28	d-f-g-h-i	Glc-OCH, $C_4H_7NO_3$, CH_2O, H_2O	94.06513	94.0652	0.2

Table S6. NMR data of 450 Da MAA in D_2O. Chemical shift calibration with DSS.

No	δ_H	mult., *J*(Hz)	δ_C	COSY	HMBC
Core					
1	-		163.5*		-
2	-		127.5		-
3	-		163.3*		-
4a	2.75*	1.3, 17.1	38.7	6b	2, 3, 5, 6, 7
4b	3.04*			6a	2, 3, 5, 6, 7, 8
5	-		73.2		-
6a	2.84*	1.3, 17.5	36.7	4b	1, 2, 4, 5, 7
6b	3.06*			4a	1, 2, 4, 5, 7, 8
7a	3.48	10.2	75.6		4, 5, 6, Hex-1'
7b	3.78	10.2			4, 5, 6, Hex-1'
8	3.68	s	61.8		2, 8
Thr					
9	4.05	d, 4.7	67.3	3	1, 10, 11, 12
10	-		177.7		-
11	4.31	dd, 4.7, 6.5	70.5	2, 4	10, 11, 12
12	1.26	d, 6.5	22.0	3	9, 11, 12
α-D-Glc					
1'	4.95	d, 3.7; $^1J_{C1, H1}$ = 170	101.3	2'	1', 2', 3', 5'
2'	3.58	3.6, 9.9	74.0	1', 3'	3'
3'	3.74		75.5	2', 4'	1', 2', 4'
4'	3.41	9.3, 9.6	72.1	3', 5'	3', 5', 6'
5'	3.63	2.2,	74.8	4', 6a', 6b'	1', 3', 4'
6a'	3.75		63.1	5', 6b'	1', 5', 6'
6b'	3.85	2.2, 12.2		5', 6a'	1', 4', 5', 6'

* = Exchangeable signals

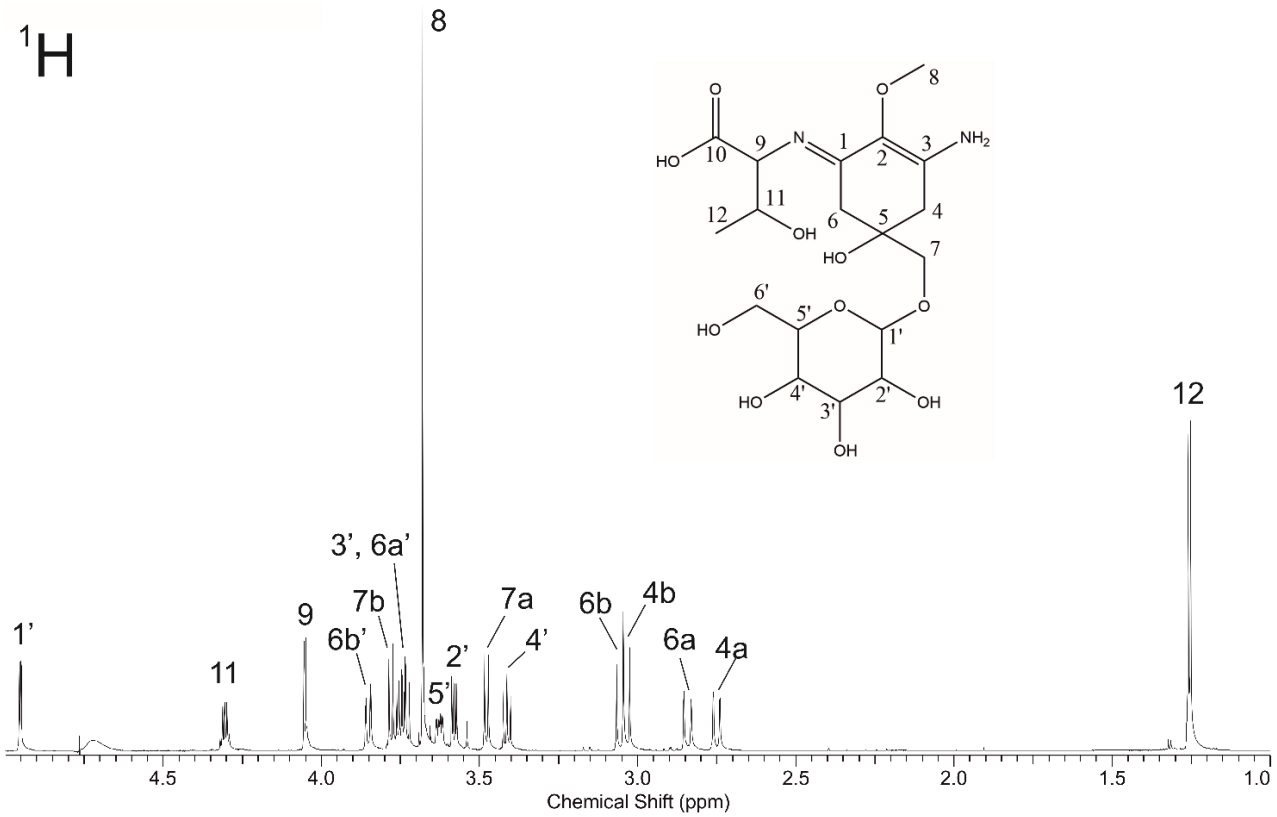

Figure S13. Annotated proton spectrum of 450 Da MAA in D_2O.

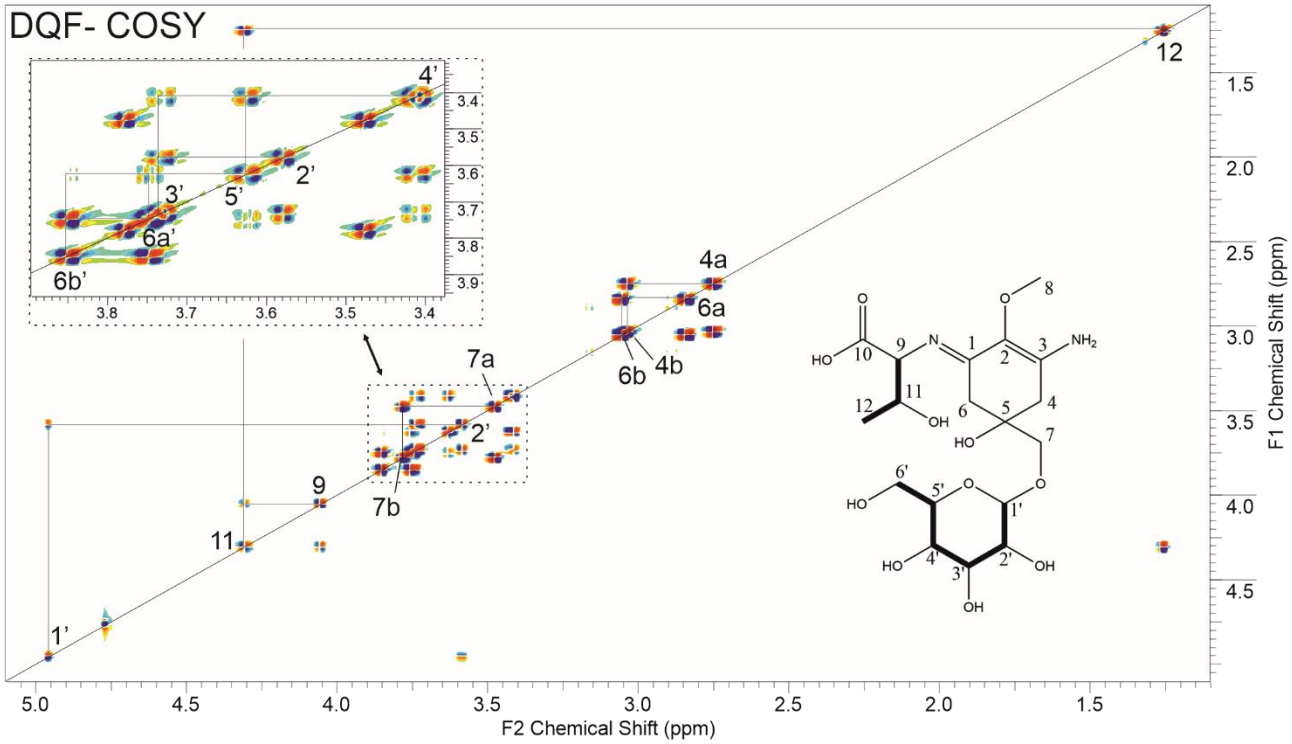

Figure S14. Annotated ^1H-^1H DQF-COSY spectrum of 450 Da MAA in D_2O. COSY correlations marked with bold bonds to the structure.

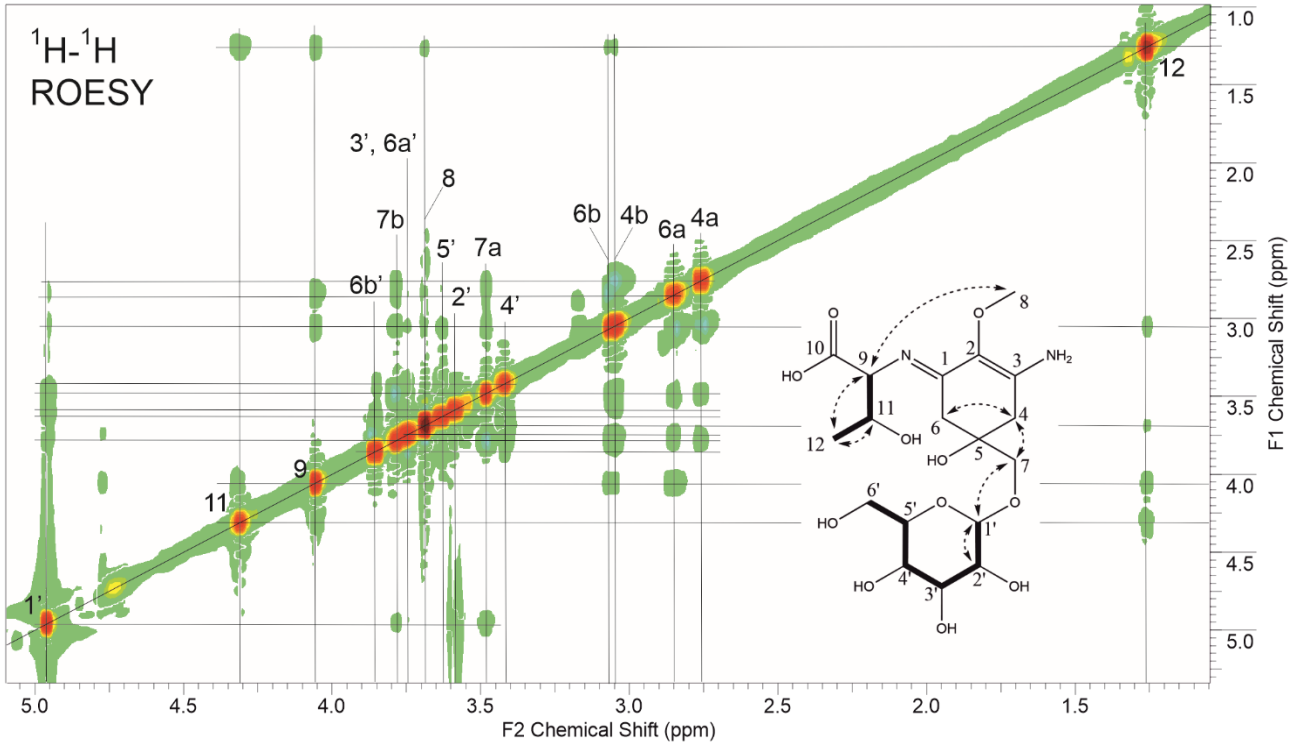

Figure S15. Annotated ^{1}H-^{1}H ROESY spectrum of 450 Da MAA in D_2O. ROESY correlations marked with dashed arrows to the structure and COSY correlations with bold bonds.

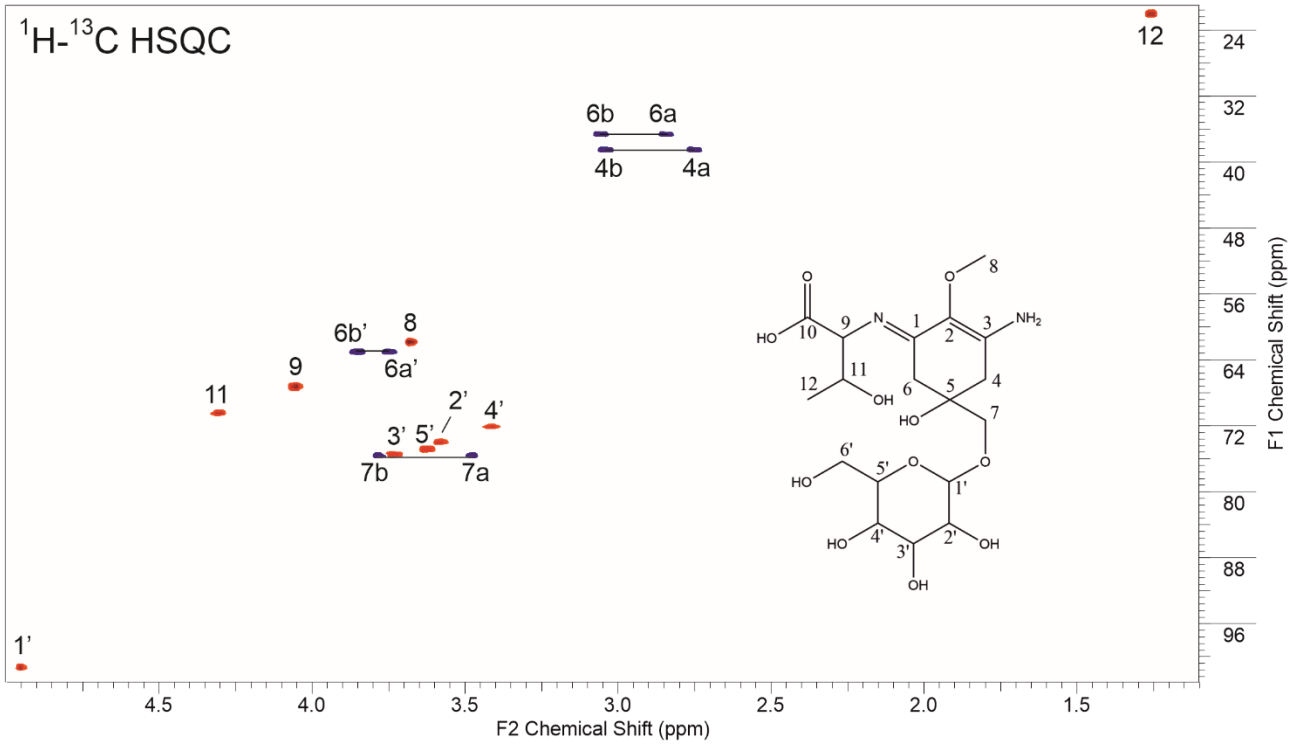

Figure S16. Annotated edited ^{1}H-^{13}C HSQC spectrum of 450 Da MAA in D_2O.

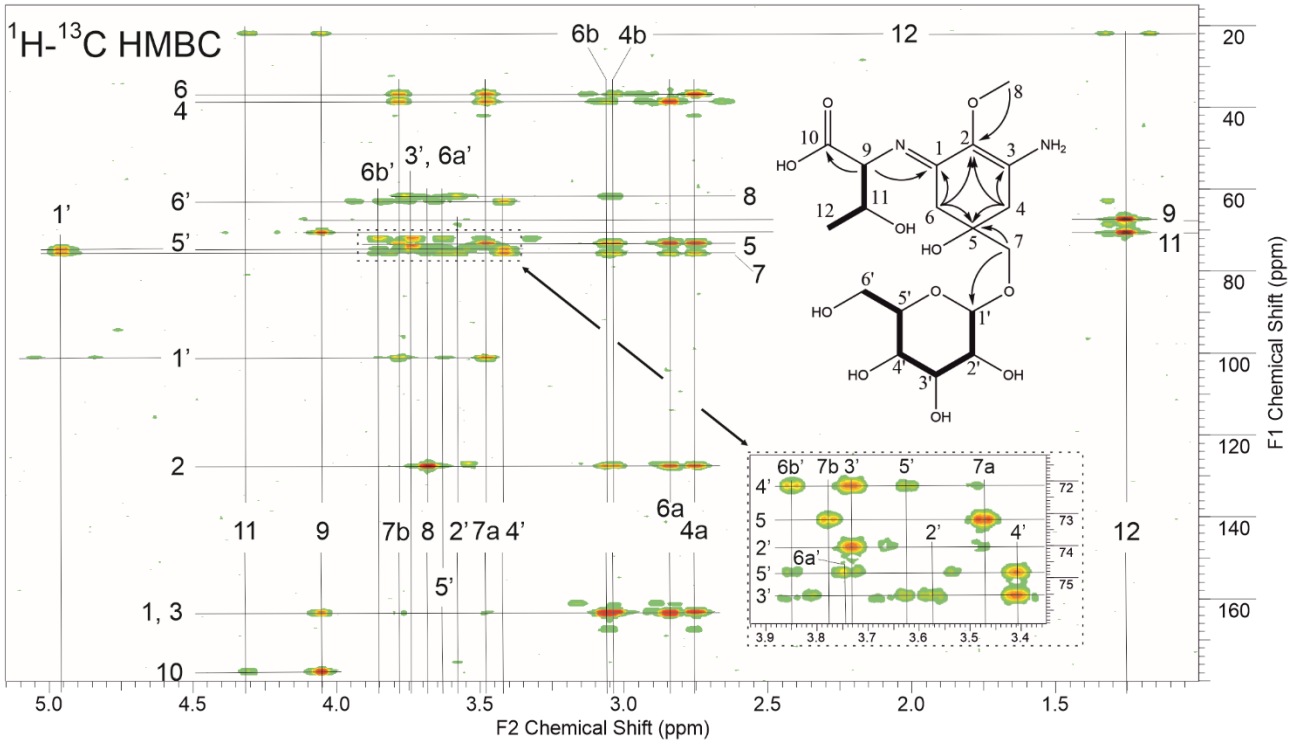

Figure S17. Annotated ^{1}H-^{13}C HMBC spectrum of 450 Da MAA in D_2O. HMBC correlations marked with arrows and COSY correlations with bold bonds to the structure.

Table S7. Complete genome assembly stats for *Nostoc* sp. UHCC 0302 (CP151099).

DNA	Size (bp)	Coverage
Chromosome	8388664	65
Plasmid 1	383299	48
Plasmid 2	358430	63
Plasmid 3	282759	71
Plasmid 4	40344	23
Plasmid 5	37423	24
Plasmid 6	33907	18
Plasmid 7	31762	25
Plasmid 8	30468	16

Table S8. MAA biosynthetic enzymes of *Nostoc* sp. UHCC 0302 (CP151099) as annotated and deposited in GenBank.

Gene name	Protein ID	Size (aa)	Product
mysA	WZF19242.1	409	Sedoheptulose-7-phosphate cyclase
mysB	WZF19243.1	277	Class-I SAM-dependent methyltransferase
mysC	WZF19244.1	465	ATP-grasp domain containing protein
$mysD_1$	WZF19246.1	348	Mycosporine-glycine-alanine ligase
mysH	WZF19248.1	297	Phytanoyl-CoA dioxygenase
$mysD_2$	WZF19974.1	345	Mycosporine-glycine-alanine ligase
$mysJ_1$	WZF19245.1	296	beta-1,6-N-acetylglucosaminyltransferase
$MysG_1$	WZF19247.1	432	Glycosyltransferase family 4 protein
$mysJ_2$	WZF19973.1	304	beta-1,6-N-acetylglucosaminyltransferase
$MysG_2$	WZF19972.1	423	Glycosyltransferase family 4 protein

Table S9. Primers used for the cloning of MAA biosynthetic gene clusters of *Nostoc* sp. UHCC 0302.

Primer Name	5'- 3' Nucleotide Sequence
P1(*mysA*_fwd)	CATGCCATGGGGTACCGAACCCAAGCAAAATATAATAAAAGGAGGTTTTTTATGAATAATGTTCAAGCATCGT
P2 (*mysD*_rev)	CGCGGATCCGCTAGCTCAATTCTGCAACACCTTTT
P3 (*mysC*+p_rev)	GTGCTCGAGTGCGGCCGCAAGCTTGTTAATCGCCATCTAATTCC
P4 (*mysJ*+p_rev)	GTGCTCGAGTGCGGCCGCAAGCTTGCTAGGATGTAATCTTATCAAGTTCATTAAGAATATTG
P5 (*mysH*_fwd)	TTGCAGAATTGAAGCGTTCAACATAGCACAG
P6 (*mysG*_rev)	GTGCTCGAGTGCGGCCGCAAGCTTGTCAAAAGGTTGTTAATTCATAG
P7 (*mysH*+p_rev)	GTGCTCGAGTGCGGCCGCAAGCTTGTTAGCAATGCAGTTCAACTC
S1 (T7 term rev)	GCTAGTTATTGCTCAGCGG
S2 (mysC_S_fwd)	CTGCCTCAATCTACAATGCC
S3 (mysD_S_fwd)	CACAAAGCCAGAGCCAAAG
S4 (mysH_S_fwd)	GACTGACTGCTTGTGAATCC
S5 (pET_S_fwd)	ATGCGTCCGGCGTAGA
X1(araBAD _ Fwd)	CTGACGCTTTTTATCGCAACTCTCTACT
X2 (t7_terminator_rev)	GATTTGTCCTACTCAGGAGAGCGTTCA
X3 (mysA_S_rev)	CACTTGGCTATTCGCAACCAC
X4 (mysH_S_fwd)	CTACTGGCCGATCCAGGG
X5 (mysC_S_fwd)	CTGCTGAAGAATCTGCAGC
X6 (mysD1_S_fwd)	CGAGCCGTGGTTCCTGGAAGC
X7 (mysD2_S_fwd)	GCCTGTTCGACTTTCGCATCG

Table S10. RBS sequences calculated for each MAA biosynthetic gene cluster enzyme of *Nostoc* sp. UHCC 0302. (*We did not calculate an individual RBS sequence for MysB as it was almost coupled with the MysA enzyme with only 4 bases in between.)

Enzyme	**RBS sequence 5' to 3'**
MysAB*	ATTCCTGCACAAGCGGGCACAGAGAAATTAAGGAGGTTTTTT
MysC	GGGGATATTCCCTCTTCACAATACTAAACCCTAAGGAGGTATTTT
$MysD_1$	TTGTTGTAATAAGTTCGCAGGAAGCTGCGATTCGGGGAGGTTTTTA
$MysD_2$	GGTTTGGTCCTTGTTCAGTTCGTTAAGGAGGTTTTTA
MysH	CCCCCAACAACGTAGGCGGGTCAGACCCGTATAAGGAGAATTTATT
$MysJ_1$	ATTATCATAACAGGATACTAAGGAGGTCAGA
$MysJ_2$	CCAGCCCTTGTACTGGGCGCATCATCGAGTAAGGAGGTAAGT
$MysG_1$	TCGCGAGAAAAAGGAGGTCGAAT
$MysG_2$	CCATCAAGAGAATAGCGCTCTTATATCCCAAAAATTAAGGAGGTTTTTTT

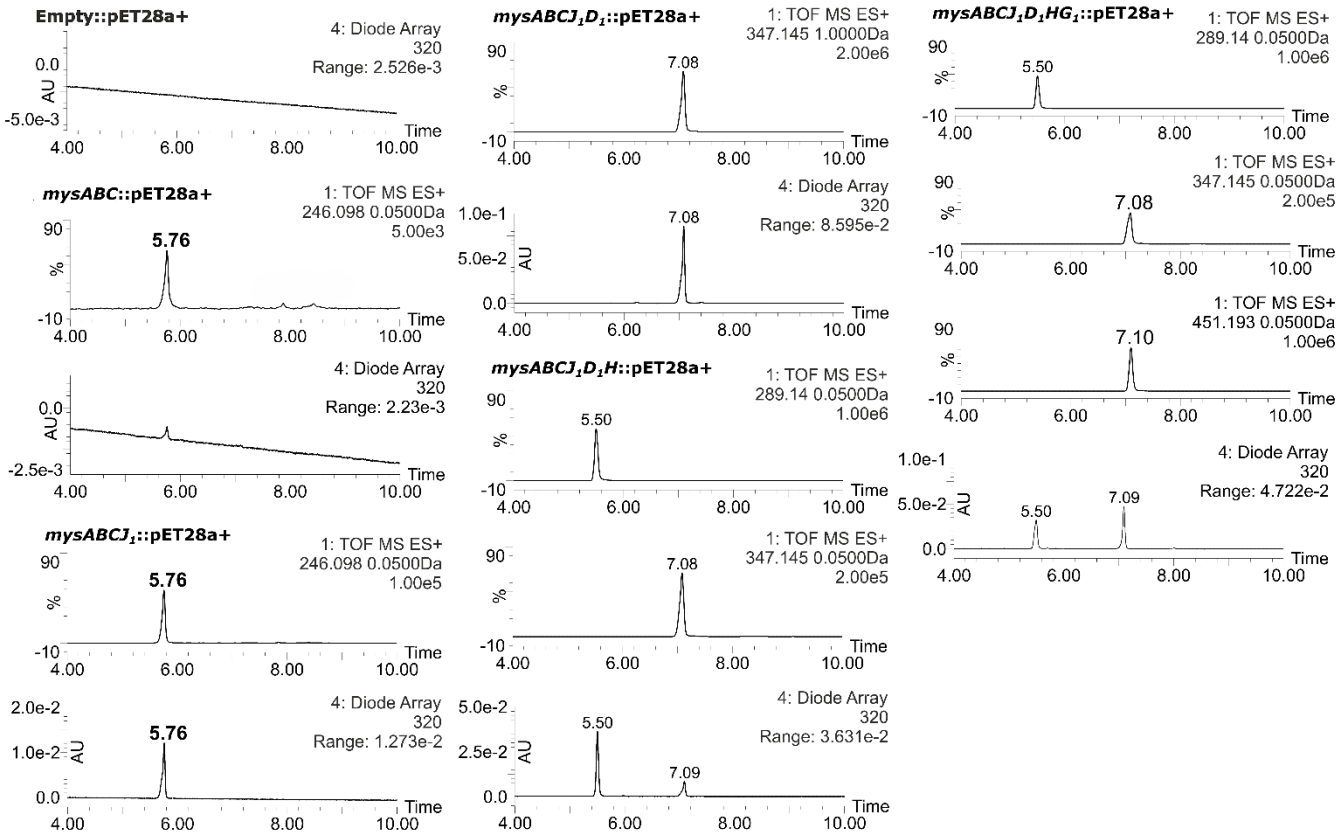

Figure S18. MS ES+ and UV chromatograms of different MAA variants detected from the extracts of recombinant *Escherichia coli* BL21 (DE3) cultures expressing different MAA biosynthetic gene cluster constructs from *Nostoc* sp. UHCC 0302 in pET28a+.

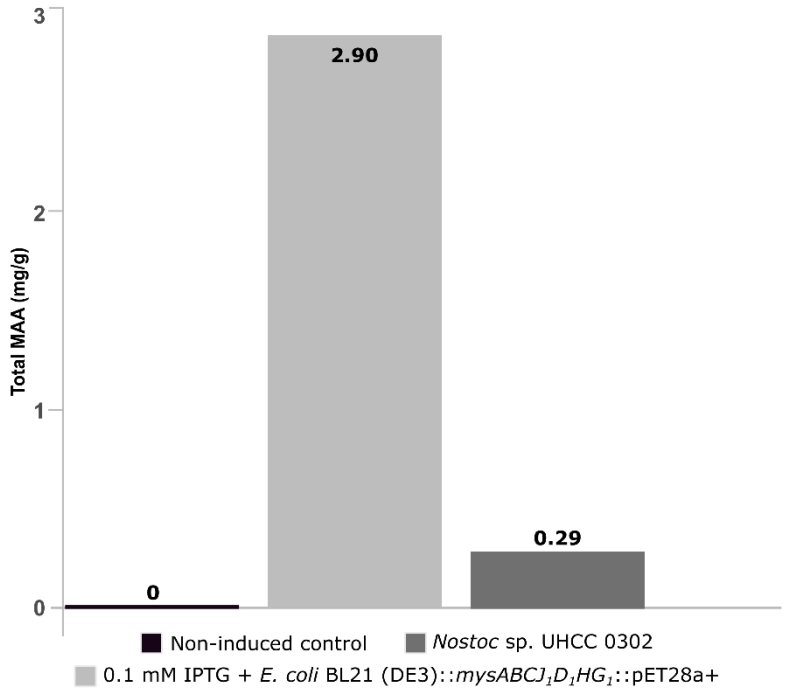

Figure S19. Total MAA concentration per dry biomass (mg/g) over 24 hours of 0.1 mM IPTG induced and non-induced production in recombinant *E. coli* clones expressing the *mysABCJ*$_1$*D*$_1$*HG*$_1$ gene cluster in pET28a+ system in LB medium supplemented with 1 % Xylose, versus the 30-day old cultures of *Nostoc* sp. UHCC 0302 grown in optimal laboratory growth conditions.

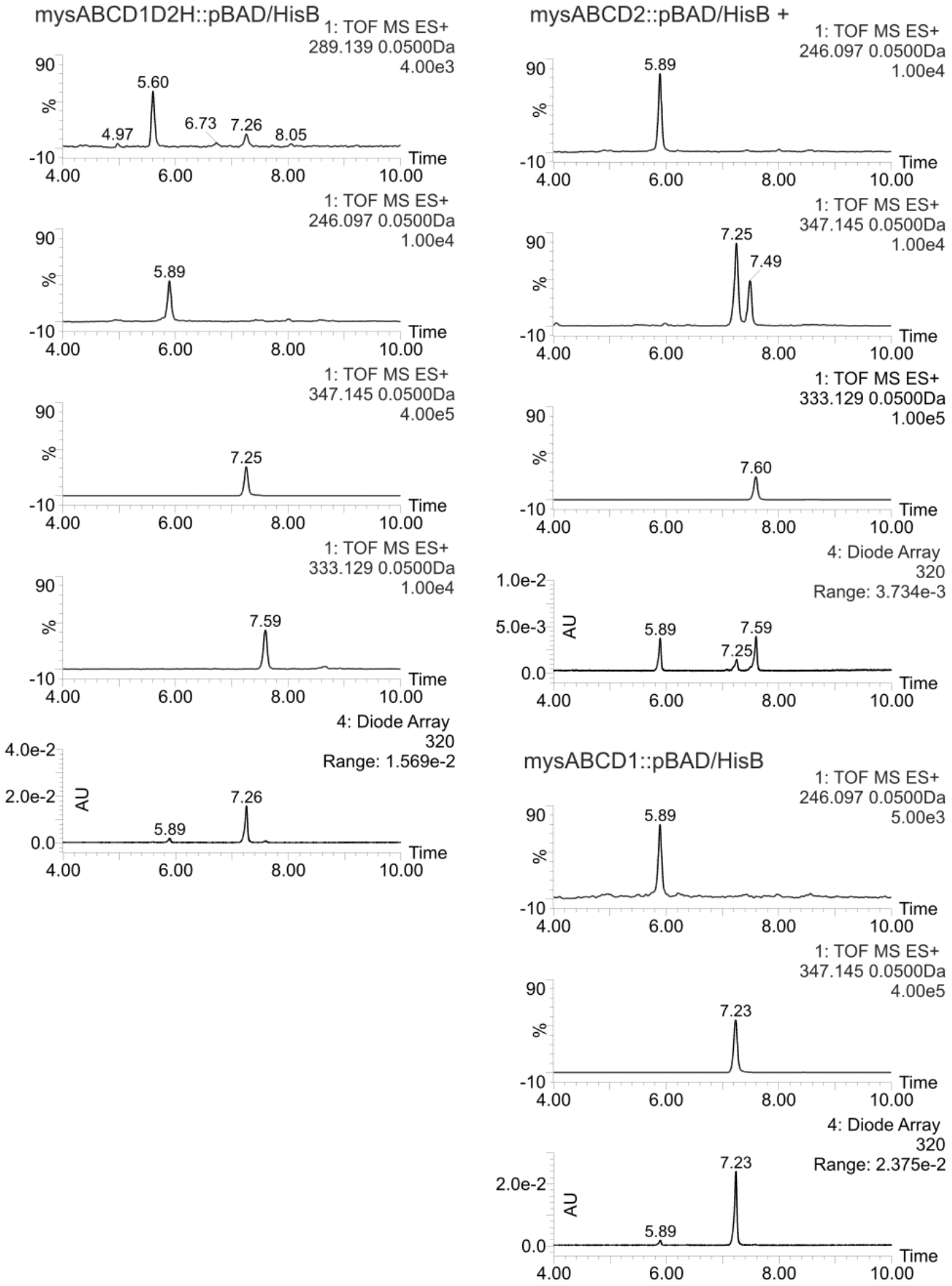

Figure S20. MS ES+ and UV chromatograms of different MAA variants detected from the extracts of recombinant *Escherichia coli* BL21 (DE3) cultures expressing different synthetic constructs of MAA biosynthetic gene cluster genes from *Nostoc* sp. UHCC 0302 in pBAD/His B.

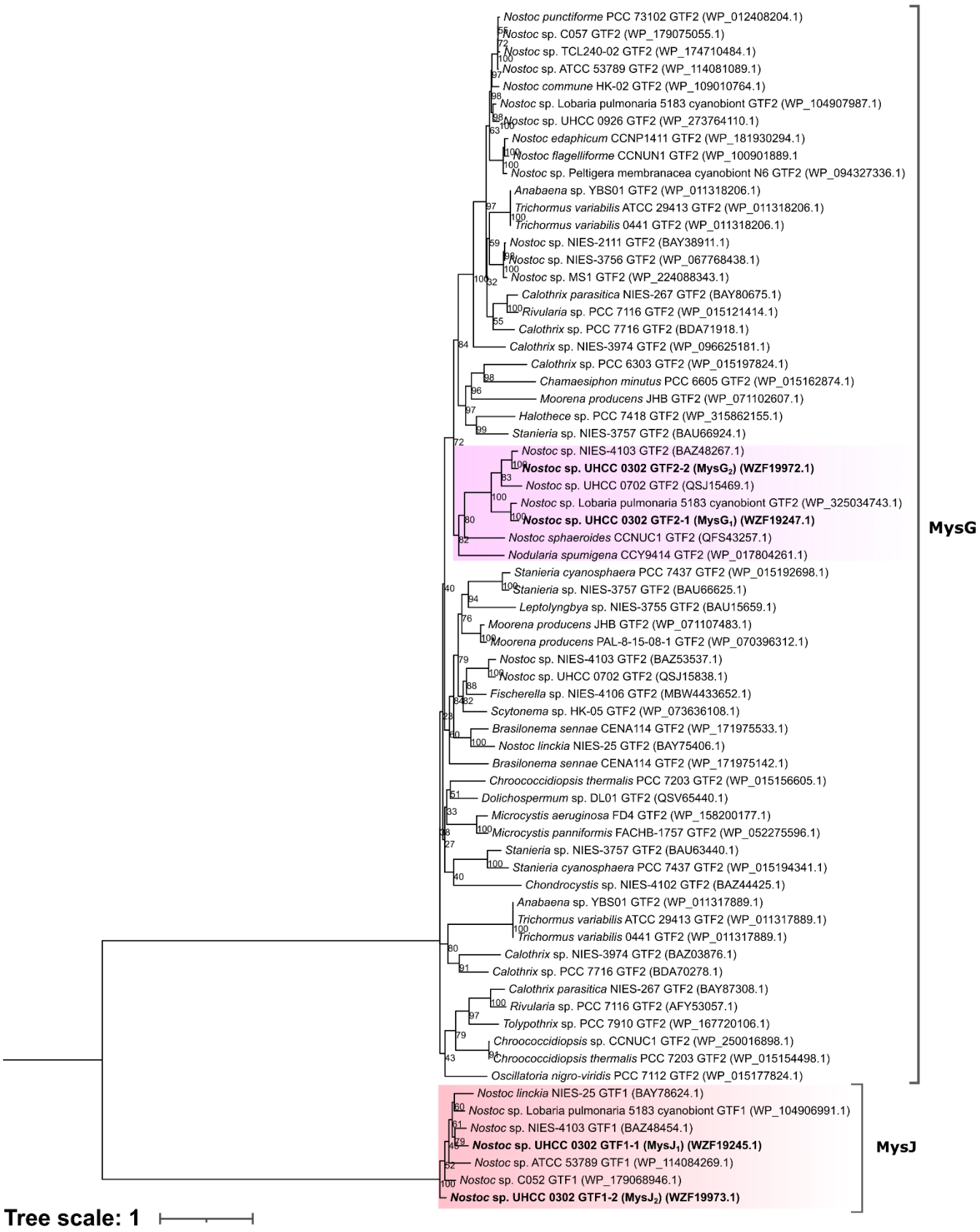

Figure S21. Phylogenetic distribution of MysJ and MysG in 52 complete cyanobacterial genomes containing a MAA biosynthetic gene cluster. Phylogenetic tree constructed using amino acid sequences of the glycosyltransferase enzymes using IQ-TREE v1.7 with the substitution model of JTTDCMut+F+I+G4. (GTF: Glycosyltransferase, GTF1: MysJ, GTF2: MysG

Table S11. Homology based protein structure prediction summary using Swiss-Model[1] for *Nostoc* sp. UHCC 0302 MysJ1/2 and MysG1/2 enzymes. NAG: 2-acetamido-2-deoxy-beta-D-glucopyranose. UDX: uridine-5'-diphosphate-xylopyranose. GLC-F6P: 6-O-phosphono-beta-D-fructofuranose-(2-1)-alpha-D-glucopyranose. UDP: uridine-5'-diphosphate. *Automatic entry from UniProt, not reviewed.

MysJ$_{1/2}$ Hits:

Code	J1/J2 Seq. Identity (%)	Method	Ligands	Oligo State	Name	Organism	Reference
A0A2A2TLA8.1.A	80.74 / 78.55	AlphaFold v2	uncharacterized	monomer	Peptide O-xylosyltransferase	*Calothrix elsteri* CCALA 953	Uniprot Entry: A0A2A2TLA8 · A0A2A2TLA8_9CYAN
6ej7.1.A	31.71 / 28.83	X-ray, 2.0 Å	1 x NAG, 1 x UDX	Hetero-dimer	Xylosyltransferase 1	Human	Briggs & Hohenester (2018) - doi.org/10.1016/j.str.2018.03.014

MysG$_{1/2}$ Hits:

Code	G1/G2 Seq. Identity (%)	Method	Ligands	Oligo State	Name	Organism	Reference
A0A1Z4S0N4.1.A*	70.12 / 90.74	AlphaFold v2	uncharacterized	monomer	A0A1Z4S0N4	*Nostoc* sp. NIES-4103	Accession (BAZ48267.1)
6kih.1.A	21.05 / 22.07	X-ray, 3.0 Å	1 x GLC-F6P, 1 x UDP	monomer	Sucrose-phosphate synthase (tll1590)	*Thermosynechococcus elongatus*	Li et al., (2020) - doi.org/10.3389/fmicb.2020.01050

1 Waterhouse, A. et al. SWISS-MODEL: homology modelling of protein structures and complexes. Nucleic Acids Res 46, W296–W303 (2018).